

Genome reannotation of the sweetpotato (*Ipomoea batatas* (L.) Lam.) using extensive Nanopore and Illumina-based RNA-seq datasets

Authors

Bei Liang[#], Yang Zhou[#], Tianjia Liu,
Mengzhao Wang, Yi Liu, ...,
Yongping Li^{*}, Guopeng Zhu^{*}

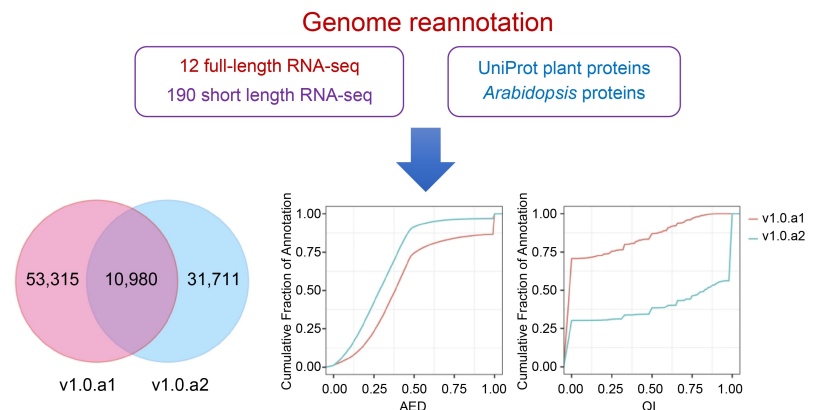
Correspondence

yplee614@hainanu.edu.cn;
zhuguopeng@hainanu.edu.cn

In Brief

This study involved the reannotation of the 'Taizhong 6' genome using extensive RNA-seq datasets and proteins sequences. The results showed a significant improvement in the completeness and accuracy of the gene structure compared to v1.0.a1, specifically in the updated v1.0.a2.

Graphical abstract




Highlights

- The updated annotation, named v1.0.a2, includes 42,751 gene models, with 97.4% complete BUSCOs.
- The updated annotation have modified or added 31,771 gene models and identified 8,736 genes with alternatively spliced isoforms.
- We have introduced a new gene ID nomenclature (IbXXGXXXXX) as an improvement over the previous nomenclature (gene.GXXXXX).

Citation: Liang B, Zhou Y, Liu T, Wang M, Liu Y, et al. 2024. Genome reannotation of the sweetpotato (*Ipomoea batatas* (L.) Lam.) using extensive Nanopore and Illumina-based RNA-seq datasets. *Tropical Plants* 3: e008 <https://doi.org/10.48130/tp-0024-0009>

Genome reannotation of the sweetpotato (*Ipomoea batatas* (L.) Lam.) using extensive Nanopore and Illumina-based RNA-seq datasets

Bei Liang^{1,2#}, Yang Zhou^{1,2#}, Tianjia Liu^{1,2}, Mengzhao Wang^{1,2}, Yi Liu^{1,2}, Yonghua Liu^{1,2}, Yongping Li^{1,2*}  and Guopeng Zhu^{1,2*}

¹ School of Breeding and Multiplication (Sanya Institute of Breeding and Multiplication), Hainan University, Sanya 572025, China

² Key Laboratory for Quality Regulation of Tropical Horticultural Crops of Hainan Province, School of Tropical Agriculture and Forestry, Hainan University, Haikou 570228, China

Authors contributed equally: Bei Liang, Yang Zhou

* Corresponding authors, E-mail: yplee614@hainanu.edu.cn; zhuguopeng@hainanu.edu.cn

Abstract

Sweetpotato (*Ipomoea batatas* (L.) Lam.) is a globally cultivated root crop of paramount significance. The hexaploid genome, known as 'Taizhong 6', has been sequenced and serves as a crucial reference genome for sweetpotato and related species within the Convolvulaceae family. However, the current annotation of the sweetpotato genome relies primarily on *ab initio* predictions and, to a lesser extent, transcriptome datasets, which only predict coding sequences. Therefore, an improved annotation is highly desirable. Here, we present a comprehensive reannotation of the sweetpotato genome, leveraging 12 Nanopore full-length RNA libraries and 190 Illumina RNA-seq libraries. The improved annotation, named v1.0.a2, includes 42,751 gene models, with 97.4% complete BUSCOs. Within this comprehensive set of gene models, we have modified or added 31,771 gene models and identified 8,736 genes with alternatively spliced isoforms. We have also introduced a new gene ID nomenclature (lbXXGXXXX) as an improvement over the previous nomenclature (gene.gXXXX). Additionally, we have annotated and provided expression levels of miRNAs and their targets at different storage roots stages. Overall, our study contributes to an updated genome annotation for the sweetpotato genome, which will significantly facilitate gene functional studies in sweetpotato and promote genomic analyses across the Convolvulaceae family.

Citation: Liang B, Zhou Y, Liu T, Wang M, Liu Y, et al. 2024. Genome reannotation of the sweetpotato (*Ipomoea batatas* (L.) Lam.) using extensive Nanopore and Illumina-based RNA-seq datasets. *Tropical Plants* 3: e008 <https://doi.org/10.48130/tp-0024-0009>

Introduction

The sweetpotato (*Ipomoea batatas* (L.) Lam) is an hexaploid species ($2n = 6x = 90$) with an estimated genome size of 2.6 G^[1]. Due to its remarkable capacity for high yield and its ability to thrive in diverse environmental conditions, the sweet potato has emerged as a cost-effective provider of essential dietary elements such as calories, protein, fiber, minerals, vitamins, and flavonoids^[2,3], particularly within developing countries. In this context, it is noteworthy that orange-fleshed sweet potatoes have emerged as pivotal players in the ongoing battle against vitamin A deficiency in Africa^[4].

The initial hexaploid sweetpotato variety to be sequenced is cultivar Taizhong 6, which was solely based on the Illumina sequencing platforms^[5]. This effort resulted in the production of 15 pseudochromosomes through the identification of gene synteny between the enhanced haplotype of the *I. batatas* assembly and the *Ipomoea nil* genome^[6]. Subsequently, with the advent of third-generation sequencing technology, the Taizhong 6 genome was resequenced using 10X Genomics techniques and Nanopore sequencing (Oxford Nanopore Technologies). The resulting long-read assembly was subsequently anchored onto chromosomes using the linkage map. This assembly effectively integrated homologous sequences into a haploid genome, measuring 473.8 Mb in size, and consisting of 15 sequences/chromosomes with an N50 length of 31 Mb. This high-quality chromosome-scaled genome provides a superior

reference for genomic and functional analyses of *I. batatas*. Using these high-quality sweetpotato genomes, candidate genes for important traits were analyzed^[7,8].

Beyond genome assembly, the availability of accurate and complete genome annotations is crucial to complement genome assembly and enhance genome applicability. Achieving this objective often involves subjecting a single genome to multiple rounds of reannotation. A notable example is the 11th annotation of the *Arabidopsis* genome, released in 2017^[9]. The advantage brought forth by Illumina technology has catalyzed the establishment of transcriptome resources for many *Ipomoea* species, particularly the cultivated relative *Ipomoea batata*^[10–12]. However, the use of short RNA-sequence reads from Illumina technology presents a significant hurdle in the process of transcript assembly and annotation^[5]. In contrast, long-read sequencing produced via Pacific BioSciences (PacBio) and Oxford Nanopore Technologies (ONT) can provide full-length transcripts, greatly enhancing the precision of gene structure annotation^[13–15]. Moreover, the adoption of full-length sequencing technology also benefits the analysis of alternative splicing, thereby enabling a more comprehensive understanding of gene expression. In the case of polyploids containing large sets of homoeologous genes, exploration of transcript splicing offers the potential to yield supplementary insights into the prevalence of subgenome dominance and the evolutionary origins of novel traits. Recently, 12 high-quality

full-length transcriptomes of *I. batata* were sequenced by ONT sequencing technology^[16]. This resource, derived from ONT RNA sequencing, presents valuable prospects for further improving *I. batata* genome annotation.

In previous studies, we successfully optimized the genome annotation pipeline to obtain high-quality gene annotations for the genomes of diploid and octoploid strawberries^[13,15,17]. To improve the annotation of the sweetpotato genome, we applied this pipeline with available RNA-seq datasets, which included 12 Nanopore full-length sequencing and 154 RNA-seq libraries. These datasets were generated from various tissues, including storage roots, leaves, and seedling tissues at distinct developmental stages or subjected to different treatments^[16,18–20]. As a result, the newly refined and enhanced annotation, designated v1.0.a2, now encompasses a total of 42,751 protein-coding genes, demonstrating an impressive completeness of 97.4%, as indicated by BUSCOs. Moreover, we identified a total of 132 known and 15 novel miRNAs and predicted their targets, in addition to providing the expression levels of these miRNAs at different storage root stages. Collectively, this updated annotation and the comprehensive gene expression profiles will serve as a valuable data resource for genomics and functional studies in sweetpotato.

Materials and methods

Transcriptome datasets used in this study

In this study, we gathered 12 ONT libraries generated from storage roots of both white-fleshed and purple-fleshed sweetpotato at different developmental stages^[16]. Additionally, we utilized 190 Illumina-based RNA-seq datasets obtained from storage roots, leaves, and seedling tissues at distinct developmental stages or subjected to different treatments^[18–20]. In addition, a total of 15 small RNA-seq libraries generated from different stages of storage root were used for small RNA identification (Supplemental Table S1)^[21].

Reads processing

The full-length reads were generated using Pychopper v2 (<https://github.com/epi2me-labs/pychopper>), which was employed to identify, orient and trim full-length Nanopore cDNA reads. Subsequently, these full-length reads were mapped to the *I. batata* genome of each sample using Minimap2 v2.24^[22]. Initially, mapped reads were then processed using cDNA Cupcake (https://github.com/Magdoll/cDNA_Cupcake) to remove redundancy, considering an alignment identity > 90% and alignment coverage > 85%. Furthermore, 5' degraded reads were excluded to obtain a final set of nonredundant reads. For Illumina reads, the first 12 bp of the Illumina RNA-seq reads were removed using the fastp tool^[23]. Subsequently, the clean reads from each library were individually aligned to the *I. batata* genome^[5] using STAR^[24]. Only the reads mapped uniquely remained for further analysis.

Comprehensive transcriptome generation

The short reads from each library were assembled into transcripts using Stringtie^[25]. To filter out weakly expressed isoforms, a minimum isoform fraction (-f) of 0.2 was applied. The resulting refined Nanopore transcripts were mapped to the *I. batata* genome using GMAP^[26] with a minimum alignment identity of > 90% and an alignment coverage of > 85%. PASA^[27] was employed to construct the best gene models based on the

aligned Nanopore full-length reads. Finally, a comprehensive transcriptome was reconstructed and generated by integrating the genome-guided short-read assembly and Nanopore full-length transcripts.

Gene structure annotation of the *I. batata* genome

The annotation of the *I. batata* genome involved the utilization of various evidence sources. Initial gene models were generated using BRAKER2^[28], which integrated trained models from BRAKER with mapped full-length reads, intron hints converted from mapped Nanopore full-length reads, intron hints derived from mapped short Illumina reads, and protein hints converted from mapped UniProt plant proteins and *Arabidopsis* proteins. Additionally, the *I. batata* genome underwent soft-repeat masking.

To obtain consensus gene models, EvidenceModeler (EVM)^[29] was used. EVM combined initial BRAKER gene models, mapped Nanopore full-length transcripts, genome-guided transcripts from Illumina RNA-seq, comprehensive transcriptome alignments from PASA, mapped UniProt proteins, and mapped *Arabidopsis* proteins. The consensus gene models were determined using a nonstochastic weighted value, with the following weight values assigned to each evidence source: 3, 6, 5, 10, 2, and 2, respectively. For further refinement of the gene models, PASA^[27] was used, incorporating the addition of alternatively spliced isoforms, UTR annotations, and modifications to the gene structure. Finally, the new annotations underwent a meticulous one-by-one manual curation, employing IGV-GSaman (v.0.6.83, <https://tbtools.cowtransfer.com/s/a11146181df14f>). This step was taken to ensure both quality assurance and accuracy.

Functional annotation of gene models

GO terms, KEGG terms, and gene functions were comprehensively annotated through the EggNOG-mapper (v.2.1.9) (<http://eggno-mapper.embl.de>). Protein sequences were submitted to both the eggNOG-mapper and KOBAS websites, and analysis was conducted using their default settings. Additionally, we employed iTAK (v.1.6, <http://itak.feilab.net/cgi-bin/itak/index.cgi>) to identify transcription factors and protein kinases.

Identification of miRNAs and their target genes

The identification of sweetpotato miRNAs followed a previously described workflow^[30,31]. Briefly, the reads obtained from the five stages of storage root^[21] were combined and processed. This involved discarding low-quality reads, trimming adapters, and collapsing identical small RNA reads using the FASTX-Toolkit (http://hannonlab.cshl.edu/fastx_toolkit). The collapsed reads were then aligned to the 'Taizhong 6' genome using Bowtie1^[32], allowing one mismatch. Subsequently, small RNAs with a length of 20–22 nucleotides and ≤ 20 genomic matches were screened for stem-loop structures, considering a maximum of four mispairings and ≤ 1 central bulge. The identified miRNAs were searched against miRbase (www.mirbase.org, v22) using BLAST to identify conserved miRNAs in plants, allowing up to two mismatches. TargetFinder 1.7^[33] was utilized to predict the target genes of the miRNAs within the v1.0.a2 gene set. Target prediction employed alignment scores up to 5, where a lower score indicated a better alignment between the miRNA and its target^[34].

Results and discussion

Reannotation of the *I. batata* genome using our prior pipeline

In this study, we carried out an updated annotation of the *I. batata* genome, denoted as version 1.0.a2 (v1.0.a2). The reannotation process of v1.0.a2 involved the integration of the Nanopore full-length transcriptome and extensive Illumina RNA-seq datasets to incorporate splice isoforms and enhance gene structure accuracy (Fig. 1). Initially, we utilized the BRAKER^[28] tool to generate an initial protein-coding gene annotation. The input data for BRAKER include BRAKER trained models, intron hints converted from aligned nanopore transcript sequences, intron hints converted from aligned RNA-seq reads, protein hints generated from mapping Araport11 and UniProt plant protein sequences, and the soft-repeat masked *I. batata* genome. The Nanopore full-length sequences were obtained from storage roots of both white-fleshed and purple-fleshed sweetpotato at different developmental stages^[16]. Illumina RNA-seq libraries were acquired from a series of different tissues in *I. batatas*, including storage roots, leaves, and seedling tissues at distinct developmental stages or subjected to different treatments^[18–20] (Supplemental Table S1). To incorporate diverse evidence sources into consensus gene models, we utilized EvidenceModeler (EVM) software^[29]. This allowed us to merge gene models predicted by BRAKER, mapped Nanopore full-length transcripts, genome-guided assembly transcripts, and mapped protein sequences (Fig. 1).

Finally, we utilized IGV-GSaman to meticulously examine the new annotations across the entire genome. Through rigorous comparisons with the mapped RNA-seq reads, we identified and selected the most accurate gene models. This meticulous process resulted in the manual curation of approximately 3000 genes, accounting for 7.01% of the total. As a result, we obtained the new annotation, v1.0.a2, which comprised a final set of 42,751 genes.

The *I. batata* annotation, designated v1.0.a2, encompasses 42,715 protein-coding genes with 63,837 transcripts, as detailed in Table 1. In a comparative analysis between v1.0.a1 and v1.0.a2, it is evident that v1.0.a2 is missing 21,544 genes present in v1.0.a1. When examining the gene models between v1.0.a1 and v1.0.a2, we consistently identified a shared pool of 10,980 genes (Supplemental Table S2). However, this shared pool accounts for only 17.07% of v1.0.a1 and 25.68% of v1.0.a2. In this context, we introduce a novel gene identification format, denoted as lbXXGXXXXX. The 'lb' prefix designates *Ipomoea batatas*, while the third and fourth digits are represented by 'X', signifying the chromosome number. 'G' is indicative of a gene, and the concluding five-digit code is assigned in accordance with the ascending order from the top/north to the bottom/south of the chromosome. Table 1 presents the statistics comparing v1.0.a1 and v1.0.a2. Remarkably, a total of 32,582 genes features 3' and/or 5' untranslated regions (UTRs), collectively representing approximately 76.2% of all annotated genes. The mean count of exons per gene increased from 5.2 to 8.1. A significant feature of the new annotation is the inclusion of alternative transcripts. A total of 8,736 transcripts arising from 42,751 genes were discerned, resulting in an average of 1.5 transcript isoforms per gene locus, spanning the entire genome. Furthermore, in the v1.0.a2 annotation, a substantial number of 17,720 genes were associated with Gene Ontology (GO) terms, compared to the 17,873 genes documented in v1.0.a1, as delineated in Table 1.

Evaluation of the annotation v1.0.a2

We employed MAKER2 software^[35] to assess the consistency of gene loci with available nucleotide and protein sequence alignments, utilizing the Annotation Edit Distance (AED) and mRNA quality index (QI). Each gene was assigned an AED score between 0 and 1, where 0 represents complete consistency with the evidence, and 1 indicates complete inconsistency with the evidence. Similarly, the QI score ranged from 0 to 1, with a higher QI score indicating a higher proportion of exons that

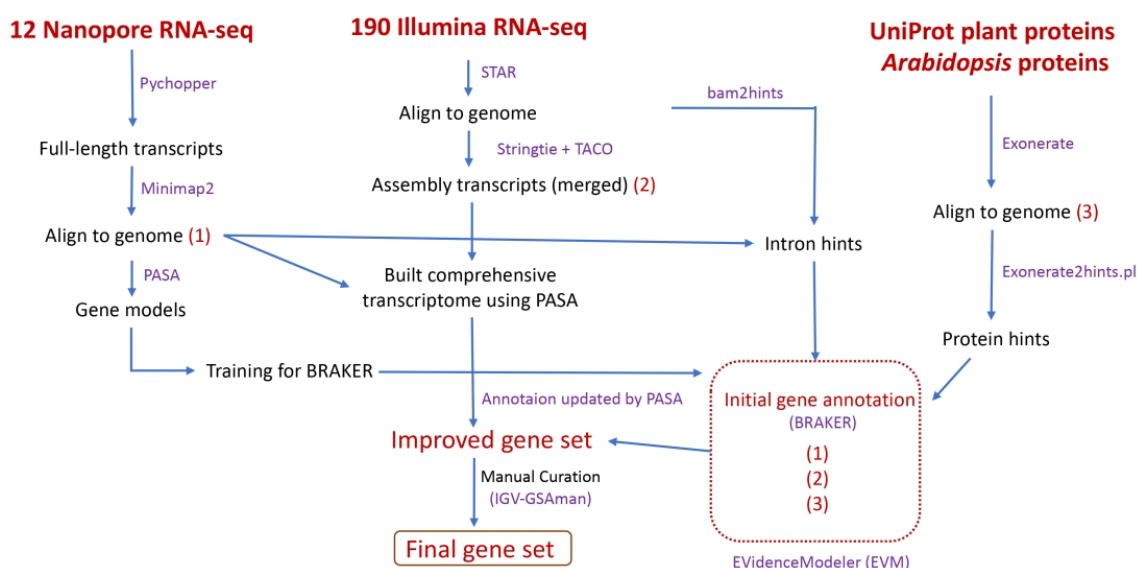


Fig. 1 Annotation workflow for *I. batata* protein-coding genes. The high-quality gene models obtained from Nanopore full-length transcripts were employed to train BRAKER. Comprehensive transcriptomes were constructed using RNA-Seq datasets through full-length and genome-guided transcripts. Additionally, *Arabidopsis* and UniProt plant protein sequences were incorporated as inputs for BRAKER. The input evidence for EvidenceModeler is highlighted within the red dotted box. Furthermore, manual curation was performed to ensure the accuracy of the annotation.

Table 1. Summary of the v1.0.a2 annotation.

Type	v1.0.a1	v1.0.a2
Protein-coding genes		
Number of genes	64,295	42,751
Mean length of genomic loci	2,498	2,953
Mean exon number	5.2	8.1
Mean CDS length	227	214
Mean length of introns	307	423
Genes with 5' UTR	–	32,220
Genes with 3' UTR	–	32,241
Genes with both 5' and 3' UTR	–	31,859
Mean 5' UTR length (bp)	–	428
Mean 3' UTR length (bp)	–	525
Number of genes with isoforms	–	8,736
Mean isoform number per gene	1.0	1.5
Genes with GO terms	17,873	17,720
Genes with functional annotations	38,602	32,629
Complete BUSCOs	89.5%	97.4%
Fragmented BUSCOs	6.0%	0.7%
Missing BUSCOs	4.5%	1.9%

matched the transcript alignment. As a result, the AED distribution analysis revealed a notable shift toward lower (improved) scores in v1.0.a2 compared with v1.0.a1 (Fig. 2b). Conversely, the cumulative QI distribution illustrated that QI scores trended toward higher (enhanced) values in v1.0.a2 when compared with v1.0.a1 (Fig. 2c). Consequently, v1.0.a2 boasts a higher percentage of gene models that enjoy robust support from transcript evidence.

To assess the completeness of the v1.0.a1 and v1.0.a2 annotations, we employed BUSCO v5.4.7^[36]. BUSCO evaluates the completeness of genome assembly and annotations by comparing them to a curated set of lineage-specific single-copy orthologs in the plantae lineage. Out of the 1,614 conserved genes examined, v1.0.a2 harbored 97.4% complete BUSCOs, while v1.0.a1 had 89.5% complete BUSCOs (Table 1). This indicates a significant enhancement in the annotation completeness of v1.0.a2 when compared to v1.0.a1.

Prediction of gene functions

To enhance the functional annotations of protein-coding genes in v1.0.a2, we subjected each predicted protein sequence to a comprehensive analysis using the InterPro protein databases using InterProScan^[37]. Next, we employed the

eggNOG mapper^[38] to assign GO categories, KEGG pathways, and functional annotation for all annotated loci. This process resulted in the precise assignment of specific GO terms to 17,265 genes, representing an increase from the 16,569 genes cataloged in v1.0.a1 (Supplemental Table S3). Additionally, we utilized the iTAK tool^[39] to identify and categorize transcription factors (TFs) and protein kinases. Within the scope of the v1.0.a2 annotation, we successfully identified a total of 2,136 TFs and 482 transcriptional regulators (TRs), as summarized in Supplemental Table S4. Notably, v1.0.a2 exhibited a higher proportion of genes encoding TFs (5.00%) than v1.0.a1 (3.84%). It is worth mentioning that despite v1.0.a2 having 21,504 fewer genes than v1.0.a1, certain transcription factor families show increases in membership, including the bZIP family from 74 to 75, the Tify family from 25 to 26, and MADS-MIKC from 24 to 46. Furthermore, v1.0.a2 contains 482 protein kinase encoding loci, which is 13 fewer than in v1.0.a1 (Supplemental Table S4).

Below, we present several examples demonstrating the enhanced accuracy of the v1.0.a2 annotation when compared to the v1.0.a1 annotation. Specifically, IB01G33760, is a homolog of GSH-induced LITAF domain protein (*ATGILP*, AT5G13190). encodes a plasma membrane-localized LITAF domain protein known to interact with LSD1 and function as a negative regulator of hypersensitive cell death^[40]. In v1.0.a2, it exhibits a newly identified translation start site and a revised gene structure (Fig. 3a). In v1.0.a2, a single gene, g4152, has been split into two separate genes, IB01G33550 and IB01G33560. Of these two genes, IB01G33550 encodes a homolog of *AtIMD2* (AT1G80560), which is one of three genes responsible for encoding the enzyme 3-isopropylmalate dehydrogenase involved in leucine biosynthesis in *Arabidopsis*^[41] (Fig. 3c). Furthermore, IB01G33270, which encodes a homolog of *AtAGL27* (AT1G77080), a MADS domain protein that functions as a negative regulator of flowering^[42,43]. Initially, it was annotated as three separate genes (Fig. 3b). All of these gene models were validated by PCR amplification and subsequent Sanger sequencing (Supplemental Fig. S1). The primers used for this validation process are listed in Supplemental Table S5.

Annotation of miRNAs and their target genes

To annotate the miRNAs within the Taizhong 6 genome, we processed and analyzed 15 sRNA libraries representing various stages of storage roots, adhering to a well-established protocol^[44]. The positions of miRNA genes on sweetpotato

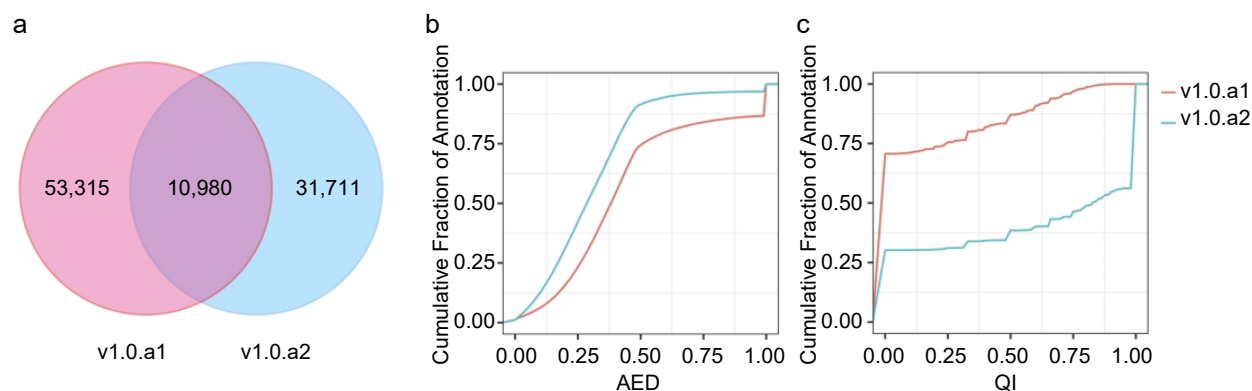


Fig. 2 Comparison of v1.0.a1 and v1.0.a2 annotation. (a) Venn diagram showing the common and unique gene structure of the CDS region between v1.0.a1 and v1.0.a2. (b) Cumulative AED distribution curves for the annotations in v1.0.a1 and v1.0.a2. (c) Cumulative QI distribution curves for the annotations in v1.0.a1 and v1.0.a2.

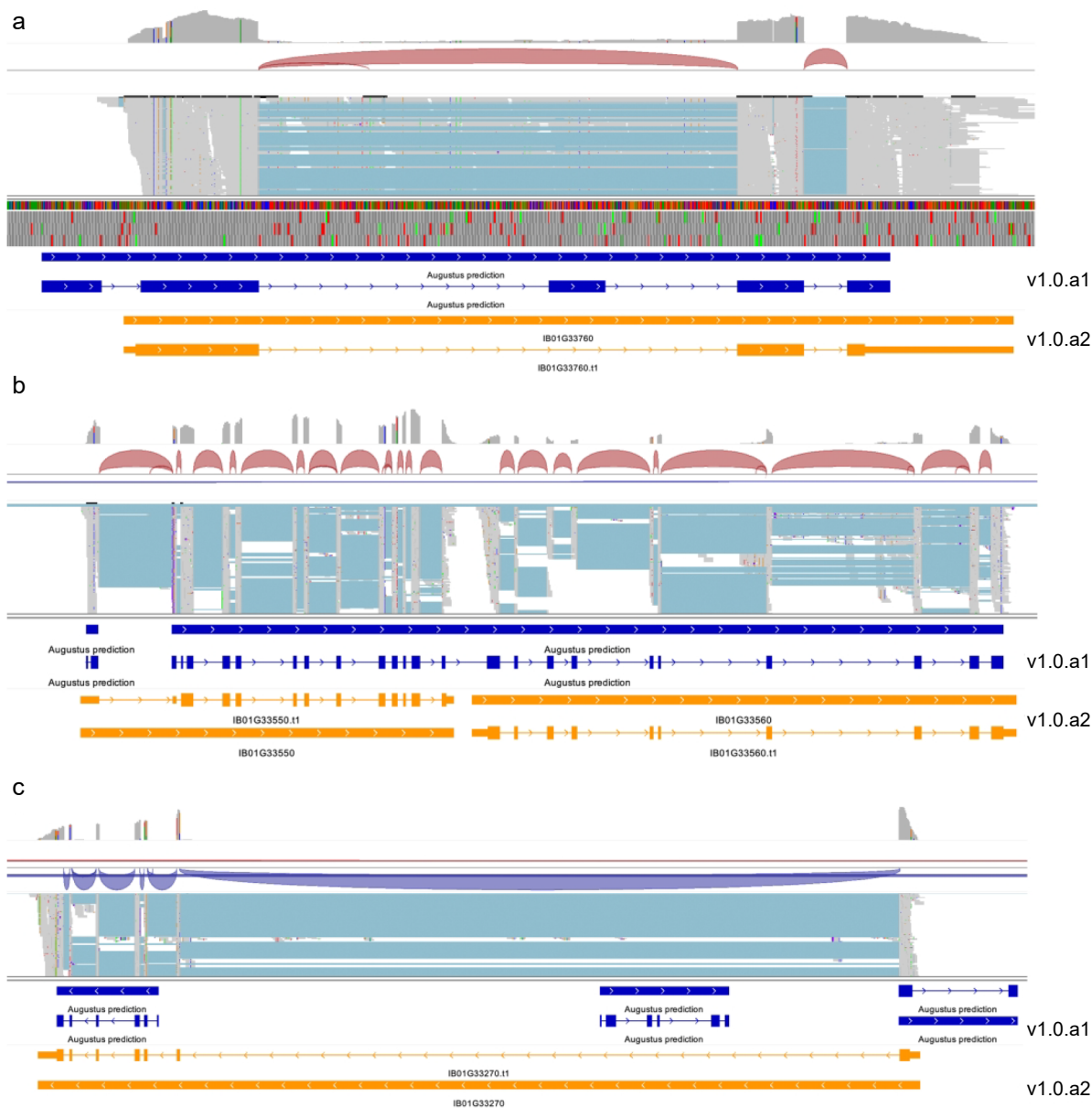


Fig. 3 Examples of known genes with improved annotations. (a) IGV view of the gene model for IB01G33760 has been updated in the new annotation. (b) IGV view of the RNA-seq mapped reads for the two adjacent genes (IB01G33550 and IB01G33560) with modified gene models in v1.0.a2 are compared to those in v1.0.a1. (c) In v1.0.a2, three genes from v1.0.a1 have been merged into a single gene, now identified as IB01G33270.

chromosomes can be observed in GFF3 file and visually represented using TBtools^[45] (Fig. 4a). Our investigation unveiled a total of 132 conserved miRNA genes, encompassing 57 unique miRNA sequences that belong to 29 known miRNA families (Fig. 4a). Furthermore, applying rigorous criteria established in previous research^[44], we identified 17 miRNAs as novel miRNAs. These miRNAs have not been characterized or annotated before, and we have designated them as fve-miRN1 to miRN17 (Fig. 4a, Supplemental Table S6). These conserved and novel miRNA genes exhibited a nonuniform distribution across the seven chromosomes (Fig. 4a).

After identifying miRNAs from 15 sweetpotato sRNA libraries, we generated an expression matrix (calculated as reads per 10 million, RP10M) of all miRNAs across different stages of sweetpotato storage roots (Supplemental Table S6). To elucidate the

expression patterns of these miRNAs in various tissues (spanning five different stages from 15 libraries), we created heatmaps for both known and novel miRNAs using hierarchical clustering and Z-score normalization (Fig. 5). Consequently, we compiled a list of miRNA targets supported by TargetFinder^[46], and these can be found in Supplemental Table S7. In total, 402 target genes have the potential to be recognized by 29 conserved miRNA families, while 172 genes are targeted by 15 novel miRNAs. It is worth noting that the presence of UTRs in the v1.0.a2 annotation may account for this significant difference, as miRNAs frequently target UTR regions. In fact, some genes have acquired miRNA target sites within their UTR regions. For example, *IB04G06160*, which encodes WRKY transcription factor 23 (*ibWRKY23*), possesses target sites for fve-miR395c in its 5' UTR (Fig. 4b).

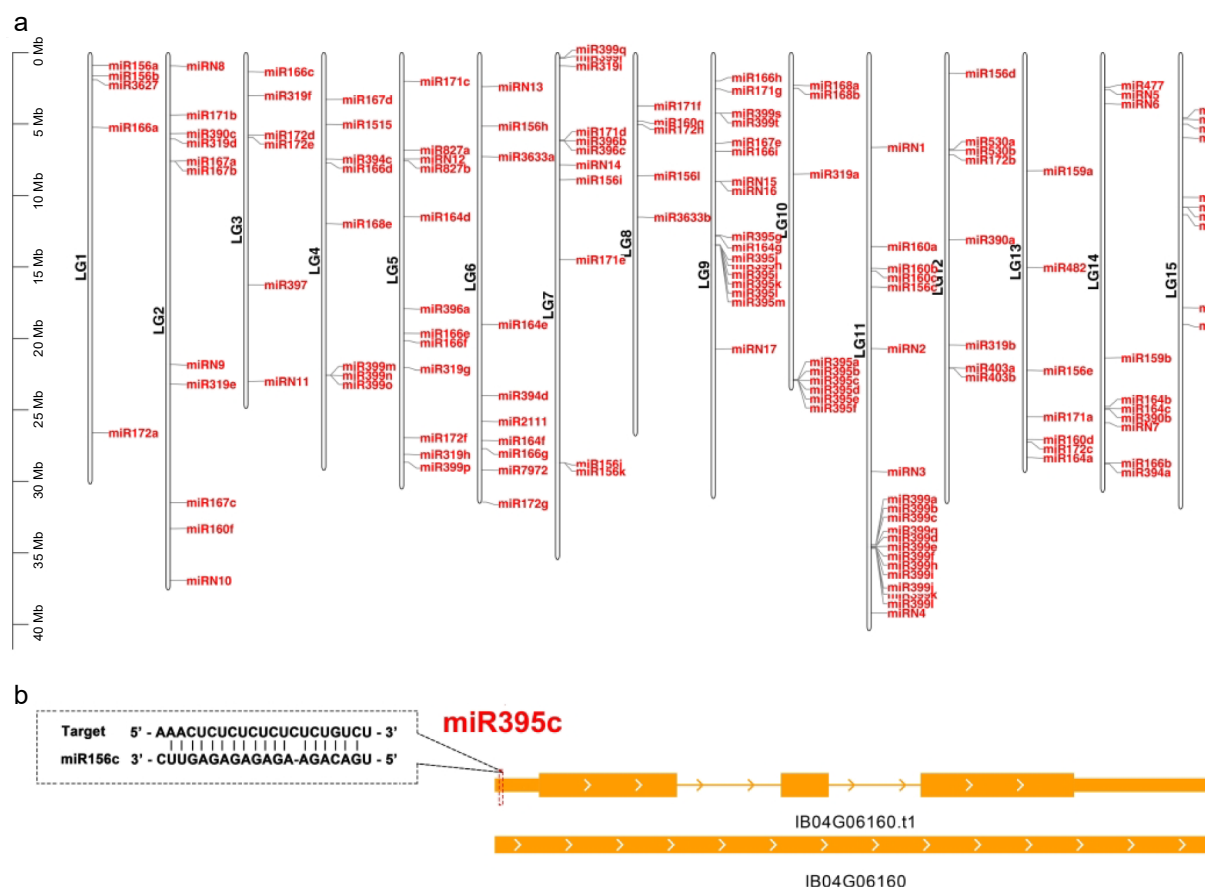


Fig. 4 Distribution of the miRNA genes in different chromosomes. (a) Distribution of the annotated miRNA genes (both known and new) in different chromosomes in the Taizhong 6 genome. (b) The target site of miR395c in IB04G06160. This gene is targeted by miR395c at the 5' UTR. The target sites are indicated by a red dashed box.

Finally, by analyzing the expression levels of all the miRNA genes across the different storage root stages (Supplemental Table S6), we have identified several miRNAs exhibited stage-specific or stage-preferential expression. For instance, miR530a was found to be specifically expressed in fibrous roots, while most miRNAs, including miR171b, miR294a, miR390, and miR403b, among others, displayed high expression levels in D1. The highly expression miRNAs in D1 may contribute to the initiation of storage root. Notably, miR168a predominantly accumulated in D3, while miR156f, miR167a, and miR397 exhibited high expression in D10. Additionally, a novel miRNA miR17 displayed a significantly high expression level in D5, indicating that this miRNA may be related to the maturation of sweetpotato storage roots.

Conclusions

In this study, we have significantly enhanced the annotation of the high-quality genome sequence assembly for hexaploid sweetpotato *I. batata*, resulting in the creation of a new annotation referred to as v1.0.a2. This comprehensive annotation process involved the utilization of 15 Nanopore long-read sequencing datasets obtained from storage roots of both white-fleshed and purple-fleshed sweetpotatoes at various developmental stages. Additionally, we incorporated data from 190 distinct Illumina short-read sequencing datasets. In this v1.0.a2 annotation, a total of 360 newly discovered genes were

successfully identified. Furthermore, we have modified or added 31,771 gene models, simultaneously incorporating transcript isoforms and expanding information on 5' and 3' untranslated regions (UTRs) in this updated annotation. Additionally, we conducted an analysis and presented miRNAs, their expression profiles across different storage root stages, and their targets. Overall, this improved annotation, v1.0.a2, represents a valuable resource for genomic analyses within the Convolvaceae family and serves as an essential reference for gene function studies in cultivated sweetpotatoes. The incorporation of newly discovered genes, refined gene models, and miRNA data enhances our understanding of sweetpotato genomics and facilitates further research in this field.

Author contributions

The authors confirm contribution to the paper as follows: study conception and design: Li Y, Liu T, Zhu G; data analysis: Liang B, Zhou Y, Liu T, Wang M, Li Y, Liu Y, Liu YH; draft manuscript preparation and revision: Li Y, Liu T, Zhu G. All authors reviewed the results and approved the final version of the manuscript.

Data availability

The gff3 file for the v1.0.a2 annotation, and the gff3 file for the miRNA annotation can be accessed at the following URL:

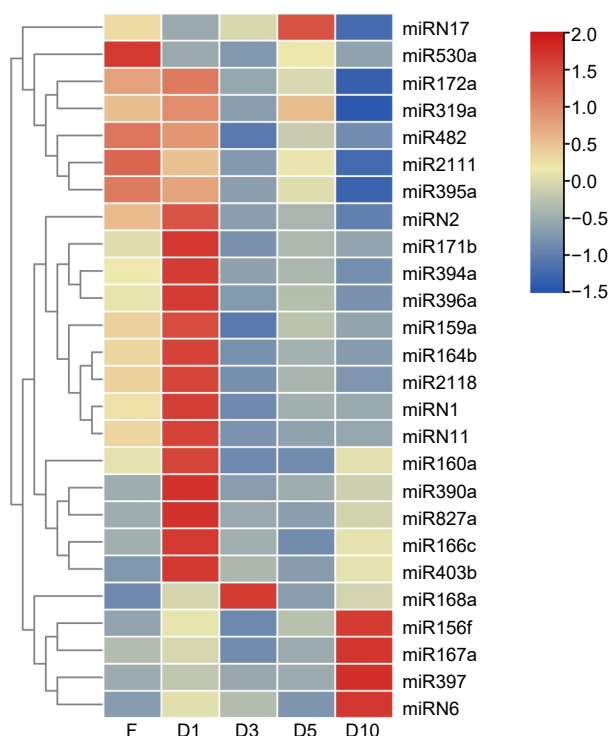


Fig. 5 Expression profiles of miRNAs in storage roots. In this figure, we present the expression profiles of miRNAs in various storage root stages: F for fibrous roots, D1 for initial storage roots (with a diameter of approximately 1 cm), D3 for storage roots (with a diameter of approximately 3 cm), D5 for storage roots (with a diameter of approximately 5 cm), and D10 for storage roots (with a diameter of approximately 10 cm). The color bar on the right side of the panel indicates the relative expression levels of miRNAs across different stages.

<https://github.com/yplee614/Sweetpotato-genome-annotation>. Additionally, the raw RNA-seq reads can be found in the NCBI Sequence Read Archive; for more details, please refer to Supplemental Table S1.

Acknowledgments

This work was supported by the Scientific Research Start-up Fund Project of Hainan University (RZ2300002728), The earmarked fund for CARS-10-Sweetpotato, the specific research fund of The Innovation Platform for Academicians of Hainan Province (YSPTZX202206), and Hainan Province Science and Technology Special Fund (ZDYF2020226).

Conflict of interest

The authors declare that they have no conflict of interest.

Supplementary information accompanies this paper at (<https://www.maxapress.com/article/doi/10.48130/tp-0024-0009>)

Dates

Received 21 October 2023; Revised 20 January 2024; Accepted 23 January 2024; Published online 21 March 2024

References

- Ozias-Akins P, Jarret RL. 1994. Nuclear DNA content and ploidy levels in the genus *Ipomoea*. *Journal of the American Society for Horticultural Science* 119:110–15
- Palumbo F, Galvao AC, Nicoletto C, Sambo P, Barcaccia G. 2019. Diversity analysis of sweet potato genetic resources using morphological and qualitative traits and molecular markers. *Genes* 10:840
- Woolfe JA. 1992. *Sweet potato: an untapped food resource*. Cambridge, New York: Cambridge University Press. <https://doi.org/10.1086/417965>
- Kurabachew H. 2015. The role of orange fleshed sweet potato (*Ipomoea batatas*) for combating vitamin A deficiency in Ethiopia: a review. *International Journal of Food Science and Nutrition Engineering* 5:141–46
- Yang J, Moeinzadeh MH, Kuhl H, Helmuth J, Xiao P, et al. 2017. Haplotype-resolved sweet potato genome traces back its hexaploidization history. *Nature Plants* 3:696–703
- Hoshino A, Jayakumar V, Nitasaka E, Toyoda A, Noguchi H, et al. 2016. Genome sequence and analysis of the Japanese morning glory *Ipomoea nil*. *Nature Communications* 7:13295
- Wang D, Liu H, Wang H, Zhang P, Shi C. 2020. A novel sucrose transporter gene *IsSUT4* involves in plant growth and response to abiotic stress through the ABF-dependent ABA signaling pathway in Sweetpotato. *BMC Plant Biology* 20:1–15
- Zhang H, Wang Z, Li X, Gao X, Dai Z, et al. 2022. The lbbBX24–lbtOE3–lbtPRX17 module enhances abiotic stress tolerance by scavenging reactive oxygen species in sweet potato. *New Phytologist* 233:1133–52
- Cheng CY, Krishnakumar V, Chan AP, Thibaud-Nissen F, Schobel S, et al. 2017. Araport11: a complete reannotation of the *Arabidopsis thaliana* reference genome. *The Plant Journal* 89:789–804
- Ji CY, Bian X, Lee CJ, Kim HS, Kim SE, et al. 2019. *De novo* transcriptome sequencing and gene expression profiling of sweet potato leaves during low temperature stress and recovery. *Gene* 700:23–30
- Lee IH, Shim D, Jeong JC, Sung YW, Nam KJ, et al. 2019. Transcriptome analysis of root-knot nematode (*Meloidogyne incognita*)-resistant and susceptible sweetpotato cultivars. *Planta* 249:431–44
- Arisha MH, Aboelnasr H, Ahmad MQ, Liu Y, Tang W, et al. 2020. Transcriptome sequencing and whole genome expression profiling of hexaploid sweetpotato under salt stress. *BMC Genomics* 21:1–18
- Li Y, Wei W, Feng J, Luo H, Pi M, et al. 2018. Genome re-annotation of the wild strawberry *Fragaria vesca* using extensive Illumina- and SMRT-based RNA-seq datasets. *DNA Research* 25:61–70
- Dong L, Liu H, Zhang J, Yang S, Kong G, et al. 2015. Single-molecule real-time transcript sequencing facilitates common wheat genome annotation and grain transcriptome research. *BMC Genomics* 16:1039
- Liu T, Li M, Liu Z, Ai X, Li Y. 2021. Reannotation of the cultivated strawberry genome and establishment of a strawberry genome database. *Horticulture Research* 8:41
- Xiong J, Tang X, Wei M, Yu W. 2022. Comparative full-length transcriptome analysis by Oxford Nanopore Technologies reveals genes involved in anthocyanin accumulation in storage roots of sweet potatoes (*Ipomoea batatas* L.). *PeerJ* 10:e13688
- Li Y, Pi M, Gao Q, Liu Z, Kang C. 2019. Updated annotation of the wild strawberry *Fragaria vesca* V4 genome. *Horticulture Research* 6:1
- Wang F, Tan WF, Song W, Yang ST, Qiao S. 2022. Transcriptome analysis of sweet potato responses to potassium deficiency. *BMC Genomics* 23:655
- Suematsu K, Tanaka M, Kurata R, Kai Y. 2020. Comparative transcriptome analysis implied a *ZEP* paralog was a key gene involved in carotenoid accumulation in yellow-fleshed sweetpotato. *Scientific Reports* 10:20607

20. Tadda SA, Li C, Ding J, Li JA, Wang J, et al. 2023. Integrated metabolome and transcriptome analyses provide insight into the effect of red and blue LEDs on the quality of sweet potato leaves. *Frontiers in Plant Science* 14:1181680
21. Tang C, Han R, Zhou Z, Yang Y, Zhu M, et al. 2020. Identification of candidate miRNAs related in storage root development of sweet potato by high throughput sequencing. *Journal of Plant Physiology* 251:153224
22. Li H. 2018. Minimap2: pairwise alignment for nucleotide sequences. *Bioinformatics* 34:3094–100
23. Chen S, Zhou Y, Chen Y, Gu J. 2018. fastp: an ultra-fast all-in-one FASTQ preprocessor. *Bioinformatics* 34:i884–i890
24. Dobin A, Davis CA, Schlesinger F, Drenkow J, Zaleski C, et al. 2013. STAR: ultrafast universal RNA-seq aligner. *Bioinformatics* 29:15–21
25. Pertea M, Pertea GM, Antonescu CM, Chang TC, Mendell JT, et al. 2015. StringTie enables improved reconstruction of a transcriptome from RNA-seq reads. *Nature Biotechnology* 33:290–+
26. Wu TD, Watanabe CK. 2005. GMAP: a genomic mapping and alignment program for mRNA and EST sequences. *Bioinformatics* 21:1859–75
27. Haas BJ, Delcher AL, Mount SM, Wortman JR, Smith RK Jr, et al. 2003. Improving the *Arabidopsis* genome annotation using maximal transcript alignment assemblies. *Nucleic Acids Research* 31:5654–66
28. Hoff KJ, Lomsadze A, Borodovsky M, Stanke M. 2019. Whole-genome annotation with BRAKER. In *Gene Prediction*, ed. Kollmar M. New York: Humana. pp. 65–95. https://doi.org/10.1007/978-1-4939-9173-0_5
29. Haas BJ, Salzberg SL, Zhu W, Pertea M, Allen JE, et al. 2008. Automated eukaryotic gene structure annotation using EvidenceModeler and the Program to Assemble Spliced Alignments. *Genome biology* 9:R7
30. Xia R, Meyers BC, Liu Z, Beers EP, Ye S, et al. 2013. MicroRNA superfamilies descended from miR390 and their roles in secondary small interfering RNA biogenesis in eudicots. *The Plant Cell* 25:1555–72
31. Xia R, Xu J, Arikait S, Meyers BC. 2015. Extensive families of miRNAs and PHAS loci in Norway spruce demonstrate the origins of complex phasiRNA networks in seed plants. *Molecular Biology and Evolution* 32:2905–18
32. Li H, Durbin R. 2009. Fast and accurate short read alignment with Burrows–Wheeler transform. *Bioinformatics* 25:1754–60
33. Meyers BC, Green PJ (eds.). 2010. *Plant microRNAs: methods and protocols*. Totowa, NJ: Humana Press. <https://doi.org/10.1007/978-1-4939-9042-9>
34. Xia R, Zhu H, An YQ, Beers EP, Liu Z. 2012. Apple miRNAs and tasiRNAs with novel regulatory networks. *Genome Biology* 13:R47
35. Holt C, Yandell M. 2011. MAKER2: an annotation pipeline and genome-database management tool for second-generation genome projects. *BMC Bioinformatics* 12:491
36. Simão FA, Waterhouse RM, Ioannidis P, Kriventseva EV, Zdobnov EM. 2015. BUSCO: assessing genome assembly and annotation completeness with single-copy orthologs. *Bioinformatics* 31:3210–12
37. Jones P, Binns D, Chang HY, Fraser M, Li W, et al. 2014. InterProScan 5: genome-scale protein function classification. *Bioinformatics* 30:1236–40
38. Powell S, Forslund K, Szklarczyk D, Trachana K, Roth A, et al. 2014. eggNOG v4.0: nested orthology inference across 3686 organisms. *Nucleic Acids Research* 42:D231–D239
39. Zheng Y, Jiao C, Sun H, Rosli HG, Pombo MA, et al. 2016. iTAK: A program for genome-wide prediction and classification of plant transcription factors, transcriptional regulators, and protein kinases. *Molecular Plant* 9:1667–70
40. Cabreira-Cagliari C, Fagundes DGS, Dias NCF, Bohn B, Margis-Pinheiro M, et al. 2018. GLP family: a stress-responsive group of plant proteins containing a LITAF motif. *Functional & Integrative genomics* 18:55–66
41. Lee SG, Nwumeh R, Jez JM. 2016. Structure and mechanism of isopropylmalate dehydrogenase from *Arabidopsis thaliana*: insights on leucine and aliphatic glucosinolate biosynthesis. *Journal of Biological Chemistry* 291(26):13421–30
42. Murphy AS, Hoogner KR, Peer WA, Taiz L. 2002. Identification, purification, and molecular cloning of N-1-naphthylphthalamic acid-binding plasma membrane-associated aminopeptidases from *Arabidopsis*. *Plant Physiology* 128:935–50
43. Jin S, Kim SY, Susila H, Nasim Z, Youn G, et al. 2022. FLOWERING LOCUS M isoforms differentially affect the subcellular localization and stability of SHORT VEGETATIVE PHASE to regulate temperature-responsive flowering in *Arabidopsis*. *Molecular Plant* 15:1696–709
44. Xia R, Ye S, Liu Z, Meyers BC, Liu Z. 2015. Novel and recently evolved microRNA clusters regulate expansive F-BOX gene networks through phased small interfering RNAs in wild diploid strawberry. *Plant Physiology* 169:594–610
45. Chen C, Chen H, Zhang Y, Thomas HR, Frank MH, et al. 2020. TBtools: an integrative toolkit developed for interactive analyses of big biological data. *Molecular plant* 13:1194–202
46. Bo X, Wang S. 2005. TargetFinder: a software for antisense oligonucleotide target site selection based on MAST and secondary structures of target mRNA. *Bioinformatics* 21:1401–2



Copyright: © 2024 by the author(s). Published by Maximum Academic Press on behalf of Hainan University. This article is an open access article distributed under Creative Commons Attribution License (CC BY 4.0), visit <https://creativecommons.org/licenses/by/4.0/>.